Proteomics

WILEY-VCH

Proteomics
Proteomics and Systems Biology

RESEARCH ARTICLE OPEN ACCESS

Toward Predicting Pandemic Potential: A Comparative Analysis of Virus-Host Interactions Between Diverse Influenza A Viruses and the Human Innate Immune System

Antoine Gerodez[1,2] | Melanie Dos Santos[3] | Mikaël Attia[3] | Killian De Geest[2] | Ibrahim Hamid[1] | Rodrigue Tesse[1] | Ilham Fdillate[1] | Marc Boschmans[2] | Steven Van Borm[2] | Mieke Steensels[2] | Benedicte Lambrecht[2] | Lionel Tafforeau[4] | Caroline Demeret[3] | Cyril Barbezange[1]

[1]Sciensano, National Influenza Centre, Brussels, Belgium | [2]Sciensano, Avian Virology and Immunology, Brussels, Belgium | [3]Institut Pasteur, Interactomics, RNA and Immunity Laboratory, Paris, France | [4]University of Mons, Cell Biology Laboratory, Mons, Belgium

Correspondence: Antoine Gerodez (antoine.gerodez@sciensano.be) | Caroline Demeret (caroline.demeret@pasteur.fr) | Cyril Barbezange (cyril.barbezange@ecdc.europa.eu)

Received: 27 October 2025 | **Revised:** 31 May 2026 | **Accepted:** 4 June 2026

Keywords: comparative analysis | influenza A virus | innate immunity | interaction networks | pandemic potential

ABSTRACT

Zoonotic infections caused by influenza A viruses (IAVs) of animal origin are a major public health concern, as they may represent the initial step toward the emergence of a pandemic strain. The host range of IAVs is shaped by species-specific virus-host interactions, and several host barriers have been identified that restrict the adaptation of avian viruses to humans. We used a comparative interaction screen by mammalian cell-based Nanoluciferase two-hybrid (mN2H) assay to investigate whether differences in the interaction networks between viral proteins from human, avian, and zoonotic IAVs and a curated panel of human innate immune factors could serve as indicators of the zoonotic potential of avian IAVs. The results revealed both conserved and strain-specific interactions, while underscoring limitations in comparing interactions across independent screens. Complementary functional analyses by siRNA knockdowns identified cellular factors and pathways potentially involved in host restriction, as well as pro-viral factors that could represent potential antiviral targets. The comparative interactomic mN2H approach holds promise for evaluating avian IAV zoonotic potential, but our findings highlighted the need for further studies using broader cellular libraries to fully validate its predictive value.

1 | Introduction

Influenza A viruses (IAVs) represent a major concern for public health [1]. IAVs are enveloped viruses whose genome consists of eight negative-sense single-stranded RNA segments coding for at least 11 viral proteins [2]. These include the surface glycoproteins hemagglutinin (HA) and neuraminidase (NA), present in the envelope together with the M2 ion channel; the viral polymerase subunits PB2, PB1, and PA; the nucleoprotein NP; the matrix protein M1; the nuclear export protein NS2; and NS1 and PA-X, which are primarily involved in innate immune evasion and/or host shut-off [2, 3]. IAVs are divided into subtypes based on the HA and NA antigenic properties. Wild aquatic birds are the natural reservoir for IAVs, carrying 17 HA (H1-16 and the recently proposed H19 [4]) and 9 NA (N1-9) subtypes. From this reservoir, IAVs can infect domestic poultry, potentially causing

Abbreviations: IAV, influenza A virus; mN2H, mammalian cell-based Nanoluciferase two-hybrid; NLR, normalized luminescent ratio; RLU, relative luminescence units. Caroline Demeret and Cyril Barbezange shared last authorship.

Significance of the Study

Influenza A viruses (IAVs) have a wide range of hosts and human infections by animal viruses raise concerns as this could lead to a pandemic. The innate immunity is the first line of defense against viral infections. Virus-host protein interactions were compared to investigate if a role for innate immunity in defining host range could be used to evaluate the zoonotic potential of avian IAVs. Although differences were observed in the interaction networks between avian and human IAVs, the results highlighted the difficulties of comparing independent screens. Functional studies based on targeted knockdown of specific cellular factors further showed that innate immune pathways might also be proviral, supporting the replication of IAVs.

devastating disease, and significant economic losses. Occasional spillover into mammals, including humans, can occur and in rare cases they can lead to the establishment of sustained transmission chains between humans. Over the past two decades, repeated spillovers of avian IAVs into humans have been reported, resulting in mild-to-fatal infections. Although these zoonotic infections rarely result in sustained human-to-human transmission, they raise public health concerns as they may represent the initial step toward human adaptation and the emergence of a pandemic strain. Since the 20th century, four influenza pandemics have been documented, and all have involved IAVs with avian origins [5]. Today, H1N1pdm09 and H3N2 subtypes circulate in the human population, causing seasonal epidemics [5]. Since 2003, zoonotic infections have mainly involved viruses of the H5N1, H7N9, and H9N2 subtypes, causing 969, 1568, and 147 reported human infections, including 464, 616, and 2 fatal cases, respectively [6, 7]. A high degree of homology was observed between internal genes of the H9N2 subtype and those of H5N1, H7N9, and H5N6, raising concerns about the role of H9N2 viruses in the emergence of avian IAVs with zoonotic potential [8].

A virus host range is determined by species-specific virus-host interactions, and several host barriers were identified to restrict the adaptation of avian IAVs to humans [9]. These barriers target the virus ability to bind to the cell, replicate within the cell, evade host restriction factors and innate immune responses, and transmit between individuals [9]. IAVs both activate and counteract host innate immune responses. Viral recognition by retinoic acid-inducible gene I (RIG-I) and Toll-like receptors (TLRs) triggers signaling pathways that activate interferon regulator factors (IRFs) 3 and 7 and nuclear factor-kappa B (NF-κB), leading to the production of type I and III interferons (IFNs), pro-inflammatory cytokines, and ultimately interferon-stimulated genes (ISGs) via the Janus kinase-signal transducer and activator of transcription (JAK-STAT) pathway [10]. On the other hand, IAVs counteract these responses through specific viral-host interactions, involving mainly the viral protein NS1 [11, 12]. Critical amino acid residues in the nucleoprotein were shown to increase avian IAV susceptibility toward myxovirus resistance protein 1 (Mx1) and butyrophilin subfamily 3 member A3 (BTN3A3) ISGs, compared to human IAVs [13, 14]. In addition, viral ribonucleoproteins (vRNPs) from avian viruses were shown to be more susceptible to direct inactivation by RIG-I than vRNPs from mammalian IAVs [15]. Despite these findings, the role of innate immune pathways in determining IAV host range remains poorly understood.

Mammalian cell-based split luciferase assays previously showed robust performance to specifically detect direct protein–protein interactions in human cells [16–18]. They identified differences in interaction patterns of the viral protein PB2 with the ubiquitin proteasome machinery that correlated with the evolution of IAVs in humans [19] and successfully correlated virus-host interaction profiles with phenotypic traits of human papillomaviruses [20]. We applied the mammalian cell, highly sensitive split Nanoluciferase enzyme-based assay (mN2H) [17] to study virus-host protein interaction differences that may act as host range barrier, hypothesizing that differences in interaction patterns could be the basis to develop in vitro tests to evaluate the degree of adaptation of animal IAV to humans. We conducted a comparative mN2H interaction screening of human innate immune factors with the internal (i.e., not present in the membrane) viral proteins from IAV subtypes of purely avian and human origin, as well as IAV subtypes that have caused zoonotic infections. Our approach identified both strain-specific and conserved interactions but highlighted the complexity of analyzing independent screens. We complemented this approach with functional studies using silencing RNAs (siRNAs) to identify host factors and pathways that may contribute to IAV host range as well as common pro-viral host factors that could represent potential antiviral targets.

2 | Methods

2.1 | Cell Lines

HEK293T, A549, MDCK, and MDCK-SIAT1 [21] cells were provided by Institut Pasteur Paris. HEK293T and A549 cells were grown in DMEM (Life Technologies cat#41965039) supplemented with 10% FBS (Life Technologies cat#10270-106), 10 U/mL penicillin and 10 µg/mL streptomycin (Life Technologies cat#15140122). MDCK and MDCK-SIAT1 cells were grown in Modified Eagle's Medium (MEM) (Life Technologies cat#31095029) supplemented with 5% FBS, 10 U/mL penicillin and 10 µg/mL streptomycin. All cell lines were grown at 37°C in 5% CO_2.

2.2 | Viruses

The screenings of the interaction between host proteins of the Innate Immunity Signaling (IIS) library and the viral proteins involved a total of eight IAV strains: for the initial screen, two seasonal IAVs currently circulating in the human population, A/Bretagne/7608/2009 (H1N1)pdm09 (called pH1N1 in Results), and A/Centre/1003/2012 (H3N2), categorized as "human" IAVs in Results; two typical avian IAVs, A/Anas Platyrhynchos/Belgium/14325/07 (H3N8) and A/Anas Platyrhynchos/Belgium/10399/2018 (H4N6), categorized as "avian" IAVs; two avian IAV subtypes associated with high zoonotic potential, A/Anhui/1-YK_RG01/2013 (H7N9) and A/chicken/Israel/1163/2011 (H9N2), categorized as "zoonotic" IAVs; and for the

independent screen, two IAVs from the H5N1 subtype, A/Gallus gallus/Belgium/16070_002/2021 (clade 2.3.4.4b) and A/chicken/Egypt/1709-6/2008 (clade 2.2.1.1), categorized as "H5N1". H5N1 clade 2.2.1.1 viruses were responsible for zoonotic infections between 2006 and 2018, in Egypt [22, 23]. Since 2021, H5N1 clade 2.3.4.4b viruses have become predominant worldwide, causing massive outbreaks in birds and dead-end infections in mammals and humans [24]. Human pH1N1 and H3N2, avian H3N8 and H4N6, zoonotic H9N2, and H5N1 clade 2.3.4.4b IAVs were used in the functional studies. The H7N9 virus was not available in our laboratories. A549-adapted pH1N1 and H3N2 strains were generated by reverse genetics, as previously described [19]. H3N8, H4N6, and H5N1 viruses were isolated in embryonated chicken eggs, while H9N2 was originally isolated in MDCK cells. All viruses were further amplified in MDCK cells, except H3N2, which was amplified in MDCK-SIAT1 cells. All virus stocks were titrated in MDCK-SIAT1 cells.

2.3 | Plasmids

Gateway-compatible destination (pDEST) vectors pN2H-N1-GW and pN2H-C2/N2-GW have been described earlier [25]. They derived from the pCINeo mammalian expression vector and, following recombinational cloning (Gateway Cloning System; Invitrogen), expressed the first (amino acid 1 to 66, Nano1 or N1) and second (amino acid 67 to 171, Nano2 or N2) parts of the Nanoluciferase in fusion to the N-terminal (pN2H-N1-GW, pN2H-N2-GW) or C-terminal ends (pN2H-C2-GW) of the viral or host proteins, respectively.

Viral protein PB2, PB1, PA, NP, M1, NS1, NS2, and PA-X ORFs were amplified directly from genomic viral RNA or intermediate plasmids containing the viral sequences, using ORF-specific Gateway primers (containing attB1.1 at the 5′ end and attB2.1 at the 3′ end) with (M1) or without (PB2, PB1, PA, NP, NS1, NS2, PA-X) STOP codons. The amplified ORFs were cloned by in vitro Gateway-based recombination into donor vectors (pDONR207/221/223). The resulting viral entry clones were transferred, via Gateway-based recombination, into pN2H-C2-GW (PB2, PB1, PA, NP, NS1, NS2, PA-X) or pN2H-N2-GW (M1) to generate plasmids expressing the viral protein fused to N2 at viral protein C-terminus (PB2, PB1, PA, NP, NS1, NS2, PA-X) or N-terminus (M1). The ORFs encoding factors of the IIS library and the random reference set (RRS) were obtained as Gateway entry plasmids from the human ORFeome collection v8.1 (https://horfdb.dfci.harvard.edu/index.php?page=home) and transferred into Gateway pDEST pN2H-N1-GW to produce N1-IIS/RRS-expressing plasmids. All entry clones were verified by Sanger sequencing (Eurofins, Germany).

2.4 | Coverage of the IIS in KEGG Pathways

The IIS factor list (Table S1) was analyzed against the KEGG database (release 110.0) in RStudio software v2024.12.0, using the function "enrichKEGG" of the clusterProfiler package v4.8.3. KEGG innate immunity-related pathways were selected based on literature.

2.5 | Mammalian Cell-Based NanoLuc Luciferase Two-Hybrid (mN2H) Assay

The mN2H was performed as previously described [25]. Briefly, HEK293T cells were transfected, in duplicate (separate plates, biological replicates), with plasmids encoding an IIS or RRS factor fused to Nano1 and a viral protein fused to Nano2. Control experiments included N1-IIS or N1-RRS plasmids combined with an empty N2 plasmid, and N2-virus plasmids combined with an empty N1 plasmid. At 24 h post-transfection (hpt), the luciferase activity was measured directly in the cells using the Nano-Glo Luciferase Assay (Promega) according to the manufacturer's protocol. In the initial screening (pH1N1, H3N2, H3N8, H4N6, H7N9, and H9N2), the luminescence was measured using a Berthold Mithras 2 LB940 luminometer with an exposure time of 2 s/well. In the H5N1 screening performed in a different institute, the luminescence was measured using the GloMax Explorer (Promega) with an exposure time of 2 s/well. Results were obtained in relative luminescence units (RLU). RRS factors were only included in the initial screen.

2.6 | mN2H Analysis

The mean of the two (biological replicate) RLU values was calculated for each IIS-viral protein–protein pair and RRS-viral protein–protein pair. A normalized luminescent ratio (NLR) was calculated as previously described [20]. For a given protein pair A and B, NLR = (N1-A + N2-B)signal/[(N1-A + empty N2)signal + (empty N1 + N2-B)signal]. A positive threshold (PT) was determined for each viral protein of each viral strain, based on the NLR distribution of the viral protein against IIS factors. The PT corresponded to the third quartile plus 1.5 times the interquartile range [PT = Q3 + (1.5 × IQR)]. Host factors with an NLR above the PT were considered as interactors.

2.7 | Generation of the Interaction Network

The initial screen interactors were integrated in an interaction network using Cytoscape 3.10.0. The IIS interactor nodes were visualized with a pie chart to show which viral strain was involved in the virus-IIS protein interactions.

2.8 | Functional Studies Using siRNA

siRNAs were purchased from Horizon Discovery (ON-TARGETplus SMARTpools and Nontargeting Control pool). The siRNA sequences were designed by Horizon Discovery (Table S2). Volumes were adjusted to obtain a siRNA final concentration of 25 nM per well. Briefly, 0.65 µL of siRNA at 5 µM was added to 24.35 µL of DharmaFECT1 transfection reagent (Horizon discovery cat#T-2001) and OptiMEM GlutaMAX medium (Life Technologies cat#51985034). The 25 µL mixture of siRNA-DharmaFECT1 was added to one well of a 96-well plate. Following 30-min incubation at room temperature, 3×10^4 A549 cells in 100 µL of DMEM supplemented with 5% FBS were seeded on top of the siRNA-transfection reagent complexes and incubated at 37°C in 5% CO_2. At 48 h post-transfection, cells

were washed and infected with 100 µL of pH1N1, H4N6, H5N1 2.3.4.4b (moi 10^{-2}), H3N2, H3N8, and H9N2 (moi 10^{-1}) at 35°C. Supernatants were collected at 24 h post-infection (hpi), and viral titers were determined by plaque assays using MDCK-SIAT1 cells [31].

2.9 | Cell Viability and Luciferase-Based Knockdown Efficiency Experiments

siRNA reverse transfection was performed as described for functional studies, except that transfection was performed in white 96-well tissue culture plates (Greiner) and 1.5×10^4 A549 cells were seeded on top of the siRNA-transfection reagent complexes. Cell viability was determined at 48 hpt using the CellTiter-Glo Luminescent Viability Assay (Promega cat#G7570) kit according to the manufacturer's instructions. To measure the siRNA-knockdown efficiency, siRNA-treated A549 cells were transfected at 24 h post-siRNA transfection with 10 ng of plasmid encoding siRNA-targeted protein fused with full-length Gaussia luciferase (pGlucFL) using lipofectamine 3000 (ThermoFisher Scientific cat#L3000001). Luciferase activity was measured 24 h later in cell lysates using the Renilla luciferase assay reagent (Promega cat#E2810). All luciferase activities were measured on a GloMax Explorer (Promega).

2.10 | Statistical Analysis

Paired Student's *t*-test was used for statistical analyses, using GraphPad Prism software v.9.00 (GraphPad Software). Differences between groups were considered statistically significant at $p < 0.05$.

3 | Results

3.1 | Generation of the IIS Library

The host protein selection to compose the IIS library was mainly based on the interaction network of the virus-associated type I interferon system described by Lotteau et al. [26]. The IIS library eventually comprised 81 human factors (Table S1), including receptors, signaling molecules, and transcription factors related to innate immune pathways. The IIS library was constructed by cloning the 81 ORFs in fusion, at their N-terminus, with the first part of the NanoLuc luciferase (N1 fragment) ORF (amino acid 1 to 66). The coverage of the innate immunity-related pathways in the IIS library was estimated using the Kyoto Encyclopedia of Genes and Genomes (KEGG) pathway database. The Toll-like and RIG-I-like receptor pathways were represented by 42 and 28 IIS factors, respectively, covering 40% of all the host factors labelled to these pathways in the KEGG database. In comparison, most other KEGG pathways, including the cytosolic DNA-sensing pathway, NOD-like receptor, IL-17, C-type lectin receptor, TNF, and NF-κB signaling pathways, were approximately 25% covered in the IIS library. The PI3K-Akt, JAK-STAT, and chemokine signaling pathways were less represented, with two, seven and 13 IIS factors, respectively, covering less than 10% of all host factors labelled to these pathways in the KEGG database (Figure 1).

3.2 | Mammalian Cell-Based N2H (mN2H) Screening of the IIS Library

For the initial screen, the IIS library was screened for interaction with eight internal viral proteins (PB2, PB1, PA, NP, M1, NS1, NS2, and PA-X) from six different IAVs, through eight mN2H experiments. The IAVs included two seasonal human IAVs (pH1N1, H3N2) referred to as "human" IAVs; two purely avian IAVs (H3N8, H4N6) referred to as "avian" IAVs; and two avian IAV subtypes associated with a high zoonotic potential (H7N9, H9N2) referred to as "zoonotic" IAVs. The results for the H9N2 subtype PB2 viral protein had to be excluded from the analysis because of the high background signal that was observed (Figure S1).

Overall, a total of 201 interactions were detected between viral proteins and IIS host factors (Figure 2A). Nearly half of these interactions (44%, 89/201) involved the viral polymerase complex subunits, with PB2 (36 interactions) accounting for the largest proportion, followed by PB1 and PA (27 and 26 interactions, respectively). Interactions involving viral proteins NS1 and PA-X, known as antagonists of the host immune response, represented 14% (28/201) and 16% (32/201) of the interactions, respectively. The remaining 26% of all detected interactions involved the viral proteins NP, NS2 and M1 (with 11, 20, and 21 interactions, respectively) (Figure 2A). Human, avian and zoonotic IAVs were equally represented among all the interactions (Figure 2B, "Global"). When looking by individual viral protein, the proportion of the three IAV categories implicated in interactions varied. Interactions with viral protein PB2 predominantly implicated human IAVs (47%), while the majority of M1 interactions implicated avian IAVs (46%). Zoonotic IAVs were proportionally more implicated in interactions with NP (45%), NS1 (42%), NS2 (40%), and PA-X (37%) (Figure 2B).

Among the total 201 interactions (edges) identified with host factors, several were shared by different IAV strains. When the IAV origin category was ignored, this led to a network of 69 edges representing distinct viral-host protein–protein pairs involving 36 different IIS host factors (Figure 2C). Twenty-one host factors were linked to only 1 viral protein, while the remaining 15 were linked to at least 2 viral proteins. Several host factors were found to occupy a central place in the interaction network, harboring interactions with five or more viral proteins. These included the heat shock protein 90 alpha family class A member 1 (HSP90AA1), which interacted with all the viral proteins except PA-X; the transcription factor IRF3, which interacted with PB1, PA, NS1, NS2, and PA-X; and the TNF receptor associated factor interacting protein (TRAIP), which interacted with PB2, NP, NS1, NS2, and PA-X. Interestingly, some host factors were also found to exclusively interact with several viral polymerase subunits: the Janus kinase 1 (JAK1) interacted with each of the three subunits PB2, PB1, PA, and the activating transcription factor 2 (ATF2) interacted with both PB2 and PB1 (Figure 2C). Adding to the analysis the distribution in IAV categories (human, avian or zoonotic) implicated in the 69 distinct edges further revealed the complexity of the network. While 29 edges connected IIS host factors with all three IAV categories (i.e., at least one strain of each category) and were classified as "common" interactions, several others were found to connect host factors with IAVs of one or

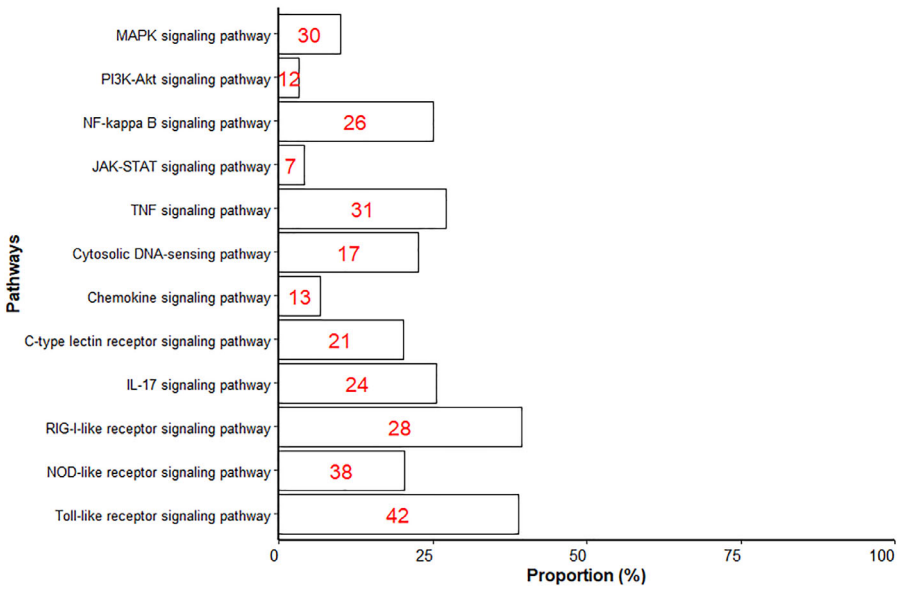

FIGURE 1 | Coverage of the Innate Immune Signaling (IIS) library in innate immune-related pathways. Host proteins composing the IIS library were mapped to innate immune KEGG pathways. Coverage is expressed as the percentage of host proteins from the IIS library that are labelled in each KEGG pathway. Numbers in red represent the number of host proteins of the IIS library mapped to the KEGG pathway.

two specific categories. Fifteen edges were exclusively found with human IAVs, eight only with zoonotic IAVs, and four were shared between human and zoonotic IAVs. Only five edges were exclusively found with avian IAVs, and four others with both avian and zoonotic IAVs. Four edges concerned both avian and human IAVs. Interactions with host factors ATF2, inhibitor of NF-κB kinase subunit alpha (IKKA), mitogen-activated protein kinase kinase 3 (MAP2K3), mitogen-activated protein kinase kinase kinase 8 (MAP3K8), mitogen-activated protein kinase 8 (MAPK8), TANK-binding kinase 1 (TBK1), and tyrosine kinase 2 (TYK2) exclusively implicated human IAVs, when those with receptor interacting serine/threonine-protein kinase 1 (RIPK1) and TIR domain-containing adaptor molecule 1 (TICAM1) were exclusive to avian IAVs, and those with heat shock protein family A (Hsp70) member 1A (HSPA1A), Fas associated via death domain (FADD), and protein activator of protein kinase R (PACT) to zoonotic IAVs. For interferon-induced protein with tetratricopeptide repeats 1 (IFIT1), NF-κB inhibitor alpha (IKBA) and epsilon (IKBE), inhibitor of NF-κB kinase subunit beta (IKKB), IRF2, IRF3, JAK1, HSP90AA1, protein inhibitor of activated STAT3 (PIAS3), relB subunit of NF-κB (RELB), TRAIP, and Unc-51 like autophagy activating kinase 1 (ULK1), the differences in IAV categories were found to depend on the viral protein involved (Figure 2C). For example, for PIAS3, the edge with NS2 concerned only a human IAV, but that with PB2 was found for all three IAV categories. Similarly, for IKBE, the edge with NS1 concerned only an avian IAV, but that with PA-X concerned all IAV categories. When also considering the interactions among factors of the IIS library, NS1 and PA-X appeared to simultaneously interact with multiple components of the canonical NF-κB pathway (Figure S2).

3.3 | Functional Impact of the Host Interactors

Thirteen host interactors were selected for preliminary functional studies. ATF2, baculoviral IAP repeat containing protein 2 (BIRC2), Tax1 binding protein 1 (TAX1BP1), and JAK1 were selected as representatives of host factors interacting with viral polymerase subunits; interleukin-1 receptor associated kinase 2 (IRAK2) and TYK2 as representatives of host factors interacting with PA-X; and TICAM1 as a representative of host factors interacting with M1. ATF2 and TYK2 also represented host factors interacting only with human strains, and TICAM1 only with avian strains. In addition, IFIT1, PIAS3, TRAIP, IKBE, RELB, and IRF2 were randomly selected among the host factors interacting with viral proteins from different IAVs. Upon small interfering RNA (siRNA)-based knockdown of these host interactors, A549 cell viability remained above 90% compared to the non-targeting (NT) siRNA-treated cells (Figure S3A), and the knockdown efficiency was above 50%. (Figure S3B). The functional impact of the 13 interactors was evaluated on the two human IAVs, the two avian IAVs, and the H9N2 zoonotic IAV used in the interaction screening. Viral titers were compared to those obtained in the NT condition (Figure S3C). Knockdown of positive control NUP62 and RAB11 host factors involved in viral mRNA export and vRNP trafficking, respectively [27, 28], led to around a one $\log_{10}$ reduction in viral titers across all strains (Figure S3D). Knockdown of TICAM1 and TYK2 impaired viral replication of all strains with viral titers reduced by 0.25 to 0.45 $\log_{10}$ for TICAM1 and 0.2 to 0.3 $\log_{10}$ for TYK2. These reductions were statistically significant only for the avian strains H3N8 and H4N6 (Figure 3). Knockdown of PIAS3 was also found to impair viral replication of all strains, but with a smaller effect (0.1 to 0.25 $\log_{10}$ titer reduction), while knockdown of ATF2, TAXBP1, TRAIP, and JAK1 was found to impair or have no effect on the viral replication of the tested strains ($\log_{10}$ titer reduction ranging from 0 to 0.5, 0 to 0.4, 0 to 0.35, and 0 to 0.3, respectively). On the contrary, knockdown of IRAK2 was found to impair viral replication of all strains ($\log_{10}$ titer reduction ranging from 0.3 to 0.85) except for the zoonotic H9N2 for which a clear increase in titer was observed (0.4 $\log_{10}$) (Figure 3). For IFIT1 and RELB, knockdown did not seem to affect viral replication, except slightly for the

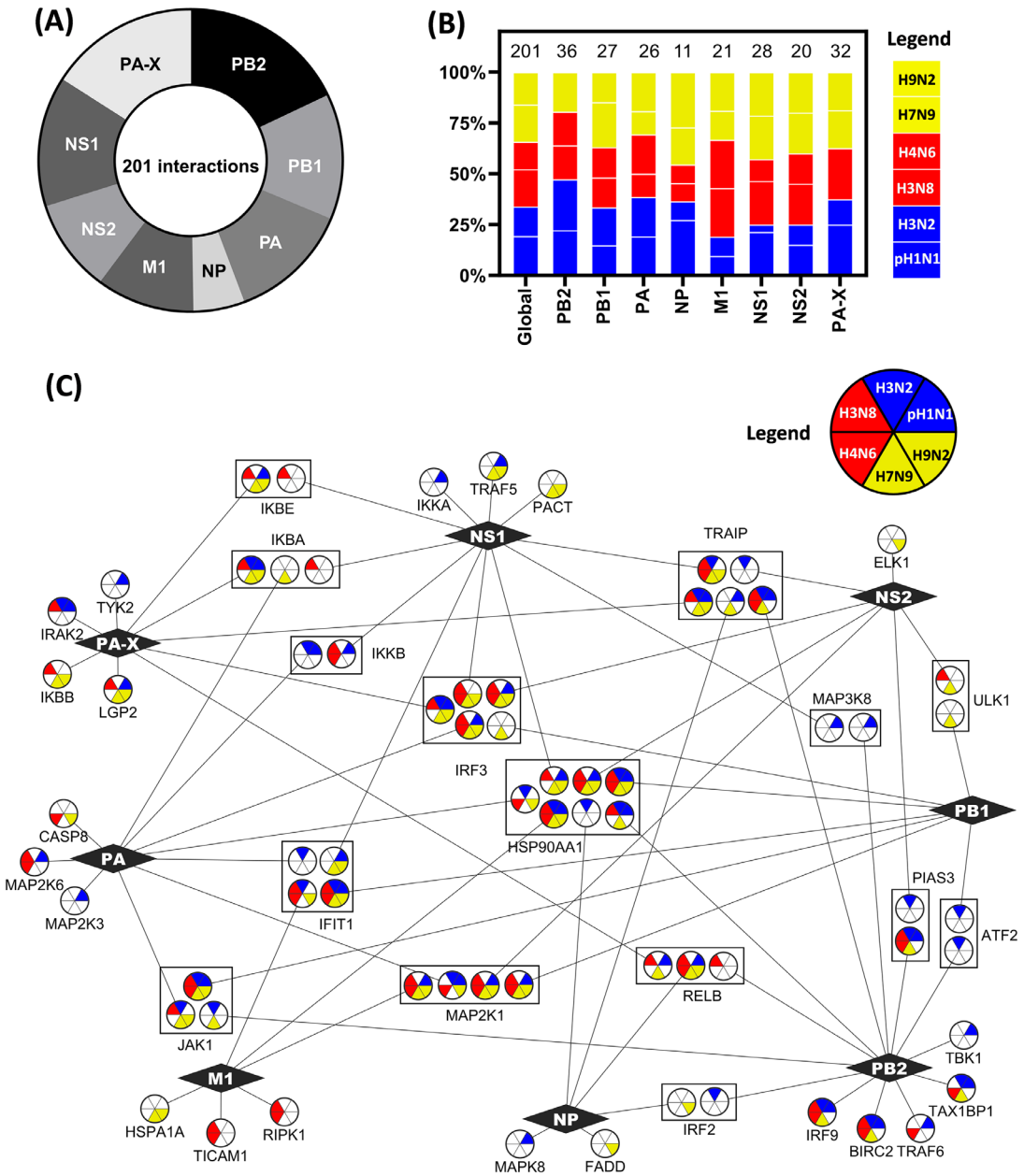

FIGURE 2 | Interactions between the IIS library and IAVs. (A) Proportion of viral proteins involved in interactions. (B) Proportion of IAV categories (human, avian, and zoonotic) involved in interactions, globally and by viral protein. H9N2 strain PB2 was not included in the analysis. (C) Interaction network between viral proteins and IIS host proteins. Viral and host proteins are represented by black diamonds and circles, respectively. Interactions are represented by edges. The IAV categories implicated in each edge are indicated by color coding.

human H3N2 virus (0.2 to 0.3 $\log_{10}$ titer reduction, significant for RELB). A similar pattern was observed for the knockdown of IKBE, but this time, viral replication of both human strains was impaired (0.25 to 0.35 $\log_{10}$ titer reduction, significant for H3N2). On the contrary, the knockdown of IRF2 was found to promote the viral replication of avian and zoonotic strains (0.15 to 0.3 $\log_{10}$ titer increase) but had little or no effect on that of human viruses. Finally, the knockdown of BIRC2 was found to impair the human H3N2 viral replication (0.4 $\log_{10}$ titer reduction), but to promote or have no effect on that of the other viruses (0 to 0.25 $\log_{10}$ titer increase, significant for pH1N1) (Figure 3).

3.4 | Independent Interaction Screening and Functional Study Comparison for H5N1 Viruses

Through an independent mN2H screening performed in a different institute, the interactions between the IIS library and internal viral proteins of two zoonotic H5N1 IAVs of different clades (2.3.4.4b and 2.2.1.1) were assessed and compared to the initial screen results (i.e., the screening with human, avian, and zoonotic IAVs in 3.2). A total of 61 interactions were detected. The proportion of interactions involving viral polymerase subunits was comparable between the H5N1 screening (Figure 4A) and the overall distribution of the initial screening (Figure 2A) (39%

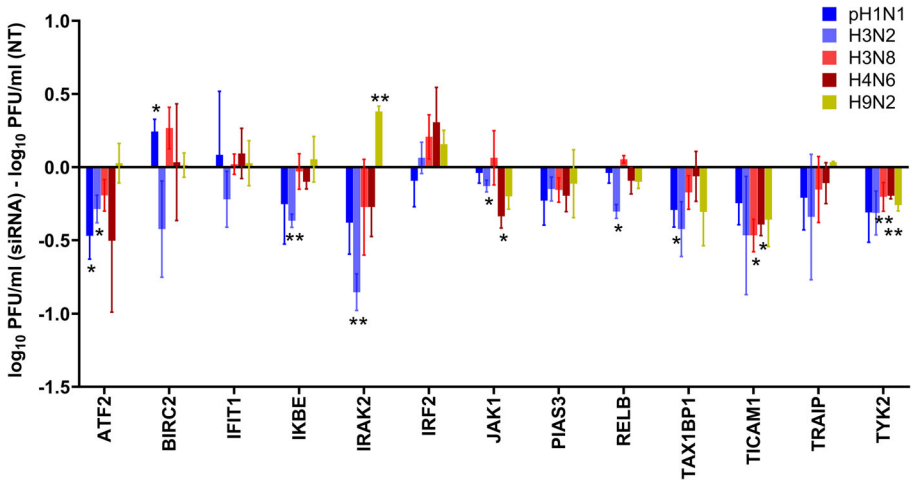

FIGURE 3 | Functional studies on a selection of host interactors. A549 cells were transfected with 25 nM non-targeting (NT) siRNA or siRNAs targeting the host factors indicated on the x-axis. At 48 hpt, cells were infected with the following viruses at the indicated moi: pH1N1, moi 10^{-2}; H3N2, moi 10^{-1}; H3N8, moi 10^{-1}; H4N6, moi 10^{-2}; H9N2, moi 10^{-1}. At 24 hpi, viral titers were determined by plaque-forming assay on MDCK-SIAT1 cells. For each virus and host factor, the $\log_{10}$ viral titer obtained under siRNA targeting conditions was compared to that obtained with NT siRNA. Results are expressed as the difference between $\log_{10}$ viral titers (siRNA−NT) and represented by mean ± SD from three independent experiments. Statistical significance was assessed for each virus and host factor by paired Student *t*-test comparing titers in siRNA versus NT conditions, using GraphPad Prism (*$p < 0.05$, **$p < 0.01$) and was represented on this figure for convenience.

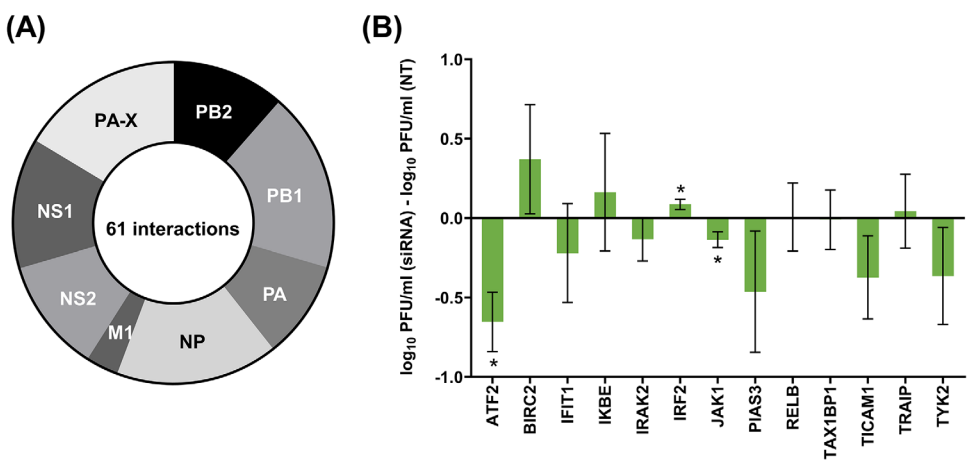

FIGURE 4 | Interactions screening and functional studies on H5N1 IAVs. (A) Proportion of viral proteins involved in interactions for the H5N1 screening. (B) Functional studies on H5N1 clade 2.3.4.4b. A549 cells were transfected with 25 nM non-targeting (NT) siRNA or siRNAs targeting the host factors indicated on the *x*-axis. At 48 hpt, cells were infected with the virus H5N1 2.3.4.4b at moi of 10^{-2}. At 24 hpi, viral titers were determined by plaque-forming assay on MDCK-SIAT1 cells. For each virus and host factor, the $\log_{10}$ viral titer obtained under siRNA targeting conditions was compared to that obtained with NT siRNA. Results are expressed as the differences between $\log_{10}$ viral titers (siRNA−NT) and represented by the mean ± SD from three independent experiments. Statistical significance was assessed for each virus and host factor by paired Student *t*-test comparing titers in siRNA versus NT conditions, using GraphPad Prism (*$p < 0.05$) and was represented on this figure for convenience.

vs. 44%). The proportion of interactions involving each viral polymerase subunits of the H5N1 viruses was similar to that obtained for the zoonotic strains in the initial screening (Figure S4). However, the H5N1 screening showed a slightly higher proportion of interactions involving PB1 (18% (11/61) vs. 14.5% (10/69)) and PB2 (11.5% (7/61) vs. 10% (7/69)), and consequently a lower proportion of interactions involving PA (10% (6/61) vs. 12% (8/69)). The proportion of interactions involving H5N1 NS2 and PA-X (11% (7/61) and 16% (10/61), respectively, Figure 4A) was found to be relatively similar to that obtained for the zoonotic strains in the initial screening (12% (8/69) and 17% (12/69) for NS2 and PA-X, respectively, Figure S4). However, the proportion of interactions involving H5N1 NS1 (13% (8/61)) was lower than that for the zoonotic strains in the initial screening (17% (12/69)). Interestingly, the H5N1 viruses strongly differed from the zoonotic strains in the initial screen for NP and M1. The proportion of interactions involving NP was much higher for H5N1 viruses (16% (10/61) vs. 7% (5/69)), but lower for M1 (3% (2/61) vs. 10% (7/69)) (Figures 4A and S4).

Out of the 29 common edges identified during the initial screening, 19 were also shared with the H5N1 category (i.e., at least one

H5N1) (Figure S5). Almost as many (18) edges were found to be unique to the H5N1 category: this is more than what was found for the zoonotic strains in the initial screening (eight edges). Only two edges were shared between the zoonotic category of the initial screening and the H5N1 category: ULK1 and PACT. Interestingly, the BIRC2-PB2 interaction that was found for all tested viruses during the initial screening was not detected in the H5N1 screening. Instead, an interaction of BIRC2 with PB1, another viral polymerase subunit, was found for one of the H5N1 viruses. As observed in the initial screening within each viral category (human, avian, zoonotic), differences were also observed between the two H5N1 viruses included in the screening (Figure S5).

Functional studies were then performed on the H5N1 clade 2.3.4.4b virus focusing on the same 13 host factors as for the initial virus strains. Knockdown of control NUP62 and RAB11A led to a more than one $\log_{10}$ decrease of the H5N1 2.3.4.4b viral titer, as observed with the other IAVs (Figure S3D). Concerning the host factors of interest, the knockdown effects on H5N1 virus replication were similar to those observed for the H9N2 zoonotic or the avian viruses, with a few exceptions (Figure 4B). For IRAK2 and IFIT1, the effect seemed to be the opposite of what was observed for the zoonotic H9N2 virus. IRAK2 knockdown had no effect or slightly impaired the H5N1 virus replication, when it was found to promote the zoonotic H9N2 replication, while IFIT1 knockdown seemed to slightly impair the H5N1 virus replication, when it had no effect on the zoonotic H9N2 virus and the avian viruses (Figure 4B).

4 | Discussion

Comparative virus-host interaction screenings have already been used to identify common and divergent interactions among homologous viral proteins, revealing shared viral strategies and potential determinants of host range and virulence, respectively [29, 30]. In the present study, mN2H assays were used for the comparative screening of interactions between the internal viral proteins of different IAV strains and a human cellular protein library focused on IIS pathways.

One of the major challenges in mN2H assays lies in the quality and exhaustiveness of the host library used. Whereas most previous interatomic studies between IAV viral proteins and the innate immunity addressed the ISGs, as the effectors of innate immunity [13, 31, 32], our approach specifically investigated the central components of the IIS pathways. This innovative approach was driven by the importance of these pathways, particularly RIG-I and TLR pathways, in restricting IAV infection [33–35], as well as the already described targeting of innate immune factors, such as RIG-I, TNF receptor-associated factor 3 (TRAF3), mitochondrial antiviral signaling protein (MAVS), IRF3 and 7, and NF-κB, by viral proteins, especially NS1, to counteract innate immune responses (reviewed in [11]). In addition, since incoming vRNPs from avian viruses were shown to be more susceptible to RIG-I inactivation compared to human virus vRNPs [15], targeting innate immune pathways more broadly may help identify host factors involved in the adaptation of avian IAVs to humans. Although our IIS library did not fully cover every KEGG-defined innate immune pathways, it included many critical signaling molecules. Notably, 30 of the 81 proteins in the IIS library ranked among the 50 most highly connected nodes in InnateDB, a curated database of innate immunity-related protein–protein interactions [36]. The library was also enriched in proteins involved in the TLR and RLR pathways, which were shown to be strongly involved in IAV antiviral response (reviewed in [11]). However, key upstream innate immune receptors, including TLRs and IFNARs, could not be included in our screen, because of the reduced efficacy of mN2H in detecting interactions involving transmembrane proteins due to the complex folding requirements associated with their transient expression [37]. Future developments in expression vector design or strategies to support correct protein folding may help to overcome this technical limitation.

From the 648 possible viral-host protein–protein pairs (edges) evaluated in the initial screen (8 distinct viral proteins × 81 host proteins), 32 interactions were previously reported in the literature (Table S3). Of these, 15 interactions were successfully recovered in our mN2H assay (recovery rate: 46%). Our mN2H thus showed similar capacity to detect interactions compared to most binary protein interaction assays for which recovery rates were estimated at around 30% [18]. Despite these solid performances, there remains room for optimization as the interactions detected in our study were not confirmed by independent interaction assays. Some mN2H studies have reported recovery rates above 70% while maintaining false positive rates near 5% [16, 17, 20]. One potential improvement would be to expand the assay to include multiple tagging configurations (i.e., N1 and N2 in N- or C-terminal of both viral and host proteins). Supporting this approach, a study showed that combining 12 different versions of N2H, differing in both tagging configurations and expression systems (i.e., mammalian, yeast, or cell-free), significantly improved sensitivity and specificity [25]. However, this multiplication of N2H versions requires high-throughput screening platforms and increases cost.

To evaluate how independent screens can be compared, we conducted an additional mN2H screen with two H5N1 strains. Forty percent of the viral-host protein–protein pairs identified in this H5N1 screen had not been detected with any of the viral strains used in the initial screening (Figure S5). While these differences may have arisen from a limit of the data analysis method from independent mN2H screens, it may also reflect actual interaction differences between strains. Consistent with this second option, an affinity purification–MS study comparing PB2, PB1, NP, and NS1 interactions across five IAV strains reported that 74% of NS1 and 40% to 50% of PB1, PB2 and NP interactions were unique to a single IAV strain [30]. Including at least one common virus strain across independent screens may help assess the impact of the analysis method on the distinct interaction patterns observed between independent screens, though this approach would increase experimental workload and cost.

IAV host range is governed by species-specific interactions between virus and host cell factors, as previously illustrated for some host factors described as barriers that avian IAVs must overcome to sustain infection in humans (reviewed in [9]). In this context, we sought to determine whether a comparative mN2H interactomic approach could be used to evaluate the

potential of avian IAV adaptation to humans, in anticipation that the method could later be applied to develop a predictive test to detect prognostic interactions, complemented for example with co-immunoprecipitation and mass-spectrometry methods. In our initial mN2H screening, with the limitation that only the factors included in the library can be considered, virus-host protein–protein pairs implicated more frequently human strains than avian and zoonotic strains, suggesting that human strains might have evolved a more intricate network of interactions with components of innate immune pathways. Interestingly, our findings suggested that the H5N1 strains may also extensively interact with the innate immune system, albeit through mechanisms distinct from those employed by human strains. This extended interaction network compared to other zoonotic IAVs may potentially help explain the repeated spillover of H5N1 in mammals and humans [38]. However, the limited number of viral strains analyzed within each category makes these interpretations largely hypothetical.

Further analysis of our mN2H screen enabled us to identify exclusive host interactors for human, avian, or zoonotic strains, potentially contributing to host range determination. However, the virus-strain specificity of mN2H-detected interactions was not clearly correlated with the effects on the viral cycle in functional assays. For example, the knockdown of ATF2, TYK2, and TICAM1 affected the replication of most or all IAVs tested, when ATF2 and TYK2 on one hand, and TICAM1 on the other hand, were found as exclusive interactors of human and avian virus strains, respectively. In contrast, the knockdown of BIRC2, an interactor of PB2 of most strains, had strain-specific effects on viral replication. These findings suggest that, under our experimental conditions, mN2H has limitations to assess the potential of avian IAV adaptation to humans. Several factors may contribute: first, mN2H may simply fail to detect certain interactions; then, some virus-host interactions may be artefactual and not essential for replication; and finally, the complexity, crosstalk and redundancy within innate immune pathways may render them less suitable for this type of comparative interactomic analysis. A similar comparative mN2H approach, focusing on alternative cellular processes, may prove more effective. For example, targeting the ubiquitin–proteasome system, where PB2 interaction patterns were shown to reflect IAV evolution in humans [19], or proteins involved in RNA decay, among which some were identified as pro-viral factors for human IAVs [39], may better reveal interaction differences that contribute to host adaptation.

In addition to network-level analysis, interatomics combined with siRNA-based functional studies can help identify cellular factors involved in the viral cycle. Several host interactors, including ATF2, JAK1, TYK2, TICAM1, TAX1BP1, and TRAIP, seemed to have a pro-viral role on most or all strains. This was quite surprising, since innate immunity is considered as an antiviral process, and results might be different with the other cellular factors of the IIS library that were not tested. However, some have already been described as pro-viral, with roles that do not seem directly related to the immune response. ATF2 is part of the AP-1 transcription family from which cJun and cFos were previously shown to support IAV replication [40, 41]. Since cFos seemed to support viral transcription [40] and ATF2 only interacted with PB2 and PB1 polymerase subunits, it could be envisaged that AP-1 transcription factors support viral polymerase activity. TYK2 and JAK1 both are tyrosine kinases involved in the JAK-STAT pathway. Several studies have found that JAK-STAT pathway components, including JAK1, JAK2, STAT1, and STAT3, seemed to support IAV replication [42–46]. Although the exact mechanism by which JAK-STAT pathway supports virus replication remains unclear, JAK1 and JAK2 were shown to phosphorylate M1, facilitating its nuclear import and virus assembly [47, 48]. JAK2-STAT3 was also proposed to enhance the expression of SREBP2 and cholesterol synthesis to promote virus replication [46]. JAK-STAT pathway may also support vRNA synthesis, since STAT1 inhibition was shown to decrease vRNA synthesis [45]. In this line, the observed interactions of JAK1 with viral polymerase subunits in our mN2H may suggest a direct role of JAK1 in supporting the viral polymerase activity. However, the JAK-STAT pathway is known to trigger the expression of antiviral ISGs [49]. In response, IAV infection was shown to induce JAK1 degradation via PB2 or cellular protein SOCS1, leading to an inhibition of innate immune responses [50, 51]. In our study, cellular factors IKBE and RELB, involved in canonical and noncanonical NF-κB pathways, respectively, appeared pro-viral only for human strains, suggesting that the effect of NF-κB on IAV may depend on virus origin. Supporting this possibility, NF-κB was previously shown to restrict avian H7N7 SC35 virus replication, while not affecting its mammalian adapted counterpart virus, the mouse-adapted SC35M [52]. Finally, host factors IRF2, IRAK2, and BIRC2 seemed to have both pro- and anti-viral activities depending on the subtype. Further investigation is required to determine whether these proteins could contribute to determining host range and it would be interesting to also include and functionally assess avian or swine orthologues in their respective host cells.

Overall, our comparative mN2H approach provided valuable insights on the complexity of the interactions between IAV and the innate immune system. Although this cannot be used at this stage as a predictive assay for pandemic potential, it identified several host factors that consistently supported replication across all IAV strains, as well as others that influenced replication in a strain-specific manner. However, the comparison of independent screens seems currently limited, leaving room for optimized methods to analyze mN2H interactomic results that could improve the robustness of the analysis across screens. Further studies using additional host libraries are also needed to fully evaluate mN2H effectiveness in assessing the potential of adaptation of avian IAVs to humans.

Author Contributions

Conceptualization: Antoine Gerodez, Cyril Barbezange, and Caroline Demeret. Investigation: Antoine Gerodez, Melanie Dos Santos, Rodrigue Tesse, Ibrahim Hamid, Ilham Fdillate, and Marc Boschmans. Formal analysis: Antoine Gerodez, Cyril Barbezange, Caroline Demeret, Lionel Tafforeau, Mikaël Attia, and Killian De Geest. Methodology: Antoine Gerodez, Cyril Barbezange, Lionel Tafforeau, Caroline Demeret, and Melanie Dos Santos. Resources: Caroline Demeret, Lionel Tafforeau, Killian De Geest, Steven Van Borm, Benedicte Lambrecht, and Mieke Steensels. Supervision: Cyril Barbezange, Caroline Demeret, Lionel Tafforeau, and Benedicte Lambrecht. Project administration: Antoine Gerodez, Cyril Barbezange, and Mieke Steensels. Visualization: Antoine Gerodez. Writing – original draft: Antoine Gerodez. Writing – review and editing: All authors. Funding acquisition: Cyril Barbezange.

Funding

The research presented in this article was funded by Sciensano as part of the PANDAI (Virus-host interaction networks to evaluate the pandemic risk of avian influenza viruses) project grant that included the financial support of A.G. as a PhD student.

Conflicts of Interest

The authors declare no conflicts of interest.

Data Availability Statement

The mammalian cell-based NanoLuc two-hybrid (mN2H) data and the virus titers obtained in the siRNA experiments have been deposited to figshare.com repository. The dataset can be found at https://figshare.com/s/870c8ad86460b4e45bcf?file=58992826.

References

1. A. D. Iuliano, K. M. Roguski, H. H. Chang, et al., "Estimates of Global Seasonal Influenza-Associated Respiratory Mortality: A Modelling Study," *Lancet* 391 (2018): 1285–1300, https://doi.org/10.1016/S0140-6736(17)33293-2.

2. N. M. Bouvier and P. Palese, "The Biology of Influenza Viruses," *Vaccine* 26, no. 4 (2008): D49–D53, https://doi.org/10.1016/j.vaccine.2008.07.039.

3. W. Hao, L. Wang, and S. Li, "Roles of the Non-Structural Proteins of Influenza A Virus," *Pathogens* 9 (2020): 812, https://doi.org/10.3390/pathogens9100812.

4. S. Fereidouni, E. Starick, K. Karamendin, et al., "Genetic Characterization of a New Candidate Hemagglutinin Subtype of influenza A Viruses," *Emerging Microbes & Infections* 12 (2023): 2225645, https://doi.org/10.1080/22221751.2023.2225645.

5. I. Wendel, M. Matrosovich, and H. D. Klenk, "SnapShot: Evolution of Human Influenza A Viruses," *Cell Host & Microbe* 17 (2015): 416, https://doi.org/10.1016/j.chom.2015.02.001.

6. European Food Safety Authority, European Centre for Disease Prevention and Control, Influenza, European Union Reference Laboratory for Avian Influenza. L. Alexakis, H. Buczkowski, M. Ducatez, et al., "Avian Influenza Overview December 2024–March 2025," *EFSA Journal* 23 (2025): 9352, https://doi.org/10.2903/j.efsa.2025.9352.

7. World Health Organization. Avian Influenza Weekly Update Number 983, 2025, https://cdn.who.int/media/docs/default-source/wpro---documents/emergency/surveillance/avian-influenza/ai_20250131.pdf?sfvrsn=5f006f99_149.

8. Y.-H. Wang, J.-J. Chen, J. Ma, et al., "Early-Warning Signals and the Role of H9N2 in the Spillover of Avian Influenza Viruses," *Med* 6 (2025): 100639, https://doi.org/10.1016/j.medj.2025.100639.

9. J. S. Long, B. Mistry, S. M. Haslam, and W. S. Barclay, "Host and Viral Determinants of Influenza A Virus Species Specificity," *Nature Reviews Microbiology* 17 (2019): 67–81, https://doi.org/10.1038/s41579-018-0115-z.

10. G. Malik and Y. Zhou, "Innate Immune Sensing of Influenza A Virus," *Viruses* 12 (2020): 755, https://doi.org/10.3390/v12070755.

11. W. An, S. Lakhina, J. Leong, K. Rawat, and M. Husain, "Host Innate Antiviral Response to influenza A Virus Infection: From Viral Sensing to Antagonism and Escape," *Pathogens* 13 (2024): 561, https://doi.org/10.3390/pathogens13070561.

12. Z. Ji, X. Wang, and X. Liu, "NS1: A Key Protein in the "Game" Between Influenza A Virus and Host in Innate Immunity," *Frontiers in Cellular and Infection Microbiology* 11 (2021): 670177, https://doi.org/10.3389/fcimb.2021.670177.

13. R. M. Pinto, S. Bakshi, S. Lytras, et al., "BTN3A3 Evasion Promotes the Zoonotic Potential of Influenza A Viruses," *Nature* 619 (2023): 338–347, https://doi.org/10.1038/s41586-023-06261-8.

14. C. M. Deeg, E. Hassan, P. Mutz, et al., "In Vivo Evasion of MxA by Avian Influenza Viruses Requires Human Signature in the Viral Nucleoprotein," *Journal of Experimental Medicine* 214 (2017): 1239–1248, https://doi.org/10.1084/jem.20161033.

15. M. Weber, H. Sediri, U. Felgenhauer, et al., "Influenza Virus Adaptation PB2-627K Modulates Nucleocapsid Inhibition by the Pathogen Sensor RIG-I," *Cell Host & Microbe* 17 (2015): 309–319, https://doi.org/10.1016/j.chom.2015.01.005.

16. P. Cassonnet, C. Rolloy, G. Neveu, et al., "Benchmarking a Luciferase Complementation Assay for Detecting Protein Complexes," *Nature Methods* 8 (2011): 990–992, https://doi.org/10.1038/nmeth.1773.

17. S. G. Choi, J. Olivet, P. Cassonnet, et al., "Maximazing Binary Interactome Mapping With a Minimal Number of Assays," *Nature Communications* 10 (2019): 3907, https://doi.org/10.1038/s41467-019-11809-2.

18. P. Braun, M. Tasan, M. Dreze, et al., "An Experimentally Derived Confidence Score for Binary Protein-Protein Interactions," *Nature Methods* 6 (2009): 91–97, https://doi.org/10.1038/nmeth.1281.

19. E. Biquand, J. Poirson, M. Karim, et al., "Comparative Profiling of Ubiquitin Proteasome System Interplay With Influenza A Virus PB2 Polymerase Protein Recapitulating Virus Evolution in Humans," *mSphere* 2 (2017): e00330–e00417, https://doi.org/10.1128/msphere.00330-17.

20. M. Muller, Y. Jacob, L. Jones, et al., "Large Scale Genotype Comparison of Human Papillomavirus E2-Host Interaction Networks Provides New Insights for E2 Molecular Functions," *PLOS Pathogens* 8 (2012): 1002761, https://doi.org/10.1371/journal.ppat.1002761.

21. M. Matrosovich, T. Matrosovich, J. Carr, N. A. Roberts, and H.-D. Klenk, "Overexpression of the α-2,6-Sialyltransferase in MDCK Cells Increases Influenza Virus Sensitivity to Neuraminidase Inhibitors," *Journal of Virology* 77 (2003): 8418–8425, https://doi.org/10.1128/jvi.77.15.8418-8425.2003.

22. G. Kayali, A. Kandeil, R. El-Shesheny, et al., "Avian Influenza A(H5N1) Virus in Egypt," *Emerging Infectious Diseases* 22 (2016): 379–388, https://doi.org/10.3201/eid2203.150593.

23. R. El-Shesheny, A. Kandeil, A. Mostafa, M. A. Ali, and R. J. Webby, "H5 Influenza Viruses in Egypt," *Cold Spring Harbor Perspectives in Medicine* 11 (2021): a038745, https://doi.org/10.1101/cshperspect.a038745.

24. A. Fusaro, B. Zecchin, E. Giussani, et al., "High Pathogenic Avian Influenza A(H5) Viruses of Clade 2.3.4.4b in Europe—Why Trends of Virus Evolution are More Difficult to Predict," *Virus Evolution* 10 (2024): veae027, https://doi.org/10.1093/ve/veae027.

25. S. G. Choi, J. Olivet, P. Cassonnet, et al., "Maximizing Binary Interactome Mapping With a Minimal Number of Assays," *Nature Communications* 10 (2019): 3907, https://doi.org/10.1038/s41467-019-11809-2.

26. V. Navratil, B. de Chassey, L. Meyniel, F. Pradezynski, C. Rabourdin-Combe, and V. Lotteau, "System-Level Comparison of Protein−Protein Interactions Between Viruses and the Human Type I Interferon System Network," *Journal of Proteome Research* 9 (2010): 3527–3536, https://doi.org/10.1021/pr100326j.

27. M. Morita, K. Kuba, A. Ichikawa, et al., "The Lipid Mediator Protectin D1 Inhibits Influenza Virus Replication and Improves Severe Influenza," *Cell* 153 (2013): 112–125, https://doi.org/10.1016/j.cell.2013.02.027.

28. A. J. Eisfeld, E. Kawakami, T. Watanabe, G. Neumann, and Y. Kawaoka, "RAB11A is Essential for Transport of the Influenza Virus Genome to the Plasma Membrane," *Journal of Virology* 85 (2011): 6117–6126, https://doi.org/10.1128/jvi.00378-11.

29. Z. Chen, C. Wang, X. Feng, et al., "Interactomes of SARS-CoV-2 and Human Coronaviruses Reveal Host Factors Potentially Affecting Pathogenesis," *EMBO Journal* 40 (2021): 107776, https://doi.org/10.15252/embj.2021107776.

30. L. Wang, B. Fu, W. Li, et al., "Comparative Influenza Protein Interactomes Identify the Role of Plakophilin 2 in Virus Restriction," *Nature Communications* 8 (2017): 13876, https://doi.org/10.1038/ncomms13876.

31. L. Martin-Sancho, S. Tripathi, A. Rodriguez-Frandsen, et al., "Restriction Factor Compendium for Influenza A Virus Reveals a Mechanism for Evasion of Autophagy," *Nature Microbiology* 6 (2021): 1319–1333, https://doi.org/10.1038/s41564-021-00964-2.

32. S. Fernbach, E. E. Spieler, I. Busnadiego, et al., "Restriction Factor Screening Identifies RABGAP1L-Mediated Disruption of Endocytosis as a Host Antiviral Defense," *Cell Reports* 38 (2022): 110549, https://doi.org/10.1016/j.celrep.2022.110549.

33. M.-L. Goulet, D. Olagnier, Z. Xu, et al., "Systems Analysis of a RIG-I Agonist Inducing Broad Spectrum Inhibition of Virus Infectivity," *PLOS Pathogens* 9 (2013): 1003298, https://doi.org/10.1371/journal.ppat.1003298.

34. M. Kandasamy, A. Suryawanshi, S. Tundup, et al., "RIG-I Signaling Is Critical for Efficient Polyfunctional T Cell Responses During Influenza Virus Infection," *PLOS Pathogens* 12 (2016): 1005754, https://doi.org/10.1371/journal.ppat.1005754.

35. D. M. Hammerbeck, G. R. Burleson, C. J. Schuller, et al., "Administration of a Dual Toll-Like Receptor 7 and Toll-Like Receptor 8 Agonist Protects Against Influenza in Rats," *Antiviral Research* 73 (2007): 1–11, https://doi.org/10.1016/j.antiviral.2006.07.011.

36. D. J. Lynn, C. Chan, M. Naseer, et al., "Curating the Innate Immunity Interactome," *BMC Systems Biology* 4 (2010): 117, https://doi.org/10.1186/1752-0509-4-117.

37. H. Hong, H.-K. Choi, and T.-Y. Yoon, "Untangling the Complexity of Membrane Protein Folding," *Current Opinion in Structural Biology* 72 (2022): 237–247, https://doi.org/10.1016/j.sbi.2021.11.013.

38. T. P. Peacock, L. Moncla, G. Dudas, et al., "The Global H5N1 Influenza Panzootic in Mammals," *Nature* 637 (2025): 304–313, https://doi.org/10.1038/s41586-024-08054-z.

39. M. Declercq, E. Biquand, M. Karim, et al., "Influenza A Virus co-opts ERI1 Exonuclease Bound to Histone mRNA to Promote Viral Transcription," *Nucleic Acids Research* 48 (2020): 10428–10440, https://doi.org/10.1093/nar/gkaa771.

40. A. Gerodez, F. E. Dufrasne, O. Denis, et al., "The Cellular Activating Protein 1 cFos Regulates Influenza A Virus Replication," *Journal of General Virology* 107 (2026): 002194, https://doi.org/10.1099/jgv.0.002194.

41. J. Xie, S. Zhang, Y. Hu, et al., "Regulatory Roles of c-jun in H5N1 Influenza Virus Replication and Host Inflammation," *Biochimica et Biophysica Acta (BBA)—Molecular Basis of Disease* 1842 (2014): 2479–2488, https://doi.org/10.1016/j.bbadis.2014.04.017.

42. J. Wang, J. Sun, J. Hu, et al., "A77 1726, the Active Metabolite of the Anti-Rheumatoid Arthritis Drug Leflunomide, Inhibits influenza A Virus Replication In Vitro and In Vivo by Inhibiting the Activity of Janus Kinases," *FASEB Journal* 34 (2020): 10132–10145, https://doi.org/10.1096/fj.201902793RR.

43. T. Watanabe, E. Kawakami, J. E. Shoemaker, et al., "Influenza Virus-Host Interactome Screen as a Platform for Antiviral Drug Development," *Cell Host & Microbe* 16 (2014): 795–805, https://doi.org/10.1016/j.chom.2014.11.002.

44. J. Han, J. T. Perez, C. Chen, et al., "Genome-Wide CRISPR/Cas9 Screen Identifies Host Factors Essential for Influenza Virus Replication," *Cell Reports* 23 (2018): 596–607, https://doi.org/10.1016/j.celrep.2018.03.045.

45. S. Zhang, C. Huo, J. Xiao, et al., "p-STAT1 Regulates the Influenza A Virus Replication and Inflammatory Response In Vitro and Vivo," *Virology* 537 (2019): 110–120, https://doi.org/10.1016/j.virol.2019.08.023.

46. J. Zhang, Y. Wu, Y. Wang, et al., "Influenza A Virus Infection Activates STAT3 to Enhance SREBP2 Expression, Cholesterol Biosynthesis, and Virus Replication," *iScience* 27 (2024): 110424, https://doi.org/10.1016/j.isci.2024.110424.

47. A. Mecate-Zambrano, S. Sukumar, and G. Seebohm, et al., "Discrete Spatio-Temporal Regulation of Tyrosine Phosphorylation Directs Influenza A Virus M1 Protein Towards Its Function in Virion Assembly," *PLOS Pathogens* (2020): 1008775, https://doi.org/10.1371/journal.ppat.1008775.

48. S. Wang, Z. Zhao, Y. Bi, L. Sun, X. Liu, and W. Liu, "Tyrosine 132 Phosphorylation of Influenza A Virus M1 Protein is Crucial for Virus Replication by Controlling the Nuclear Import of M1," *Journal of Virology* 87 (2013): 6182–6191, https://doi.org/10.1128/jvi.03024-12.

49. X. Hu, J. Li, M. Fu, X. Zhao, and W. Wang, "The JAK/STAT Signaling Pathway: From Bench to Clinic," *Signal Transduction and Targeted Therapy* 6 (2021): 402, https://doi.org/10.1038/s41392-021-00791-1.

50. Y. Du, F. Yang, Q. Wang, et al., "Influenza A Virus Antagonizes Type I and Type II Interferon Responses via SOCS1-Dependent Ubiquitination and Degradation of JAK1," *Virology Journal* 17 (2020): 74, https://doi.org/10.1186/s12985-020-01348-4.

51. H. Yang, Y. Dong, Y. Bian, et al., "The Influenza Virus PB2 Protein Evades Antiviral Innate Immunity by Inhibiting JAK1/STAT Signalling," *Nature Communications* 13 (2022): 6288, https://doi.org/10.1038/s41467-022-33909-2.

52. S. Dam, M. Kracht, S. Pleschka, and M. L. Schmitz, "The influenza A Virus Genotype Determines the Antiviral Function of NF-κB," *Journal of Virology* 90 (2016): 7980–7990, https://doi.org/10.1128/jvi.00946-16.

Supporting Information

Additional supporting information can be found online in the Supporting Information section.

Supporting File: pmic70155-sup-0001-SuppMat.pdf.